JOURNAL OF CATALYSIS 115, 430–440 (1989)

ENDOR of Perylene Radicals Adsorbed on Alumina and Silica–Alumina Powders

II. The Matrix Effects

K. S. ROTHENBERGER, H. C. CROOKHAM, R. L. BELFORD, AND R. B. CLARKSON[1]

Department of Chemistry and Illinois ESR Center, University of Illinois, Urbana, Illinois 61801

Received September 9, 1987; revised August 17, 1988

Nuclei in the environment (matrix) of perylene cation radicals formed on activated alumina and silica–alumina powders exposed to solutions of perylene in benzene solvent were probed with electron nuclear double-resonance (ENDOR) spectroscopy. Both normal and fully deuterated perylene and benzene were studied. Depending on the nature of the sample and experimental conditions, signals were detected from protons, deuterons, and aluminum-27 in the environment of the radical. A strong proton matrix signal was observed in spectra of alumina-adsorbed radicals in all preparations, indicating the presence of protons on the surface. In contrast, spectra of radicals adsorbed on silica–alumina exhibited much weaker proton matrix signals under all conditions. A deuterium matrix signal was observed with both alumina and silica–alumina surfaces (although weakly on the latter) when deuterated solvent was present. Aluminum-27 signals were seen only from samples on the alumina surface. Active site models consistent with the results are discussed. The results suggest that the radicals, although themselves similar, occupy sites of significantly different environment.

INTRODUCTION

Historically, the method of choice in studying perylene radical formation on activated oxide surfaces has been electron paramagnetic resonance (EPR) at *X*-band. In Paper I of this series (*1*), we discussed the limitations of the conventional EPR technique and showed how electron nuclear double-resonance (ENDOR) spectroscopy can be used to overcome the difficulties in measuring weak hyperfine interactions. That paper focused on the properties and identity of the *radical* formed on activated alumina and silica–alumina surfaces. Needless to say, there is also much disagreement about the nature of the radical *site*, knowledge of which could help elucidate the mechanism of radical formation.

Perylene radical formation on activated oxide surfaces was first reported over 25 years ago (*2*) and has been the subject of many studies (*2–15*). The inherent variability of this surface interface complicates any analysis and the need to study the system *in situ*, without disrupting its innate disorder, places great demands on the investigator's methods.

The uncertainties surrounding this system cannot be attributed to lack of creativity or effort by the scientific community. However, much of the evidence to date is contradictory and defies the establishment of a complete, unified model. Early workers postulated that radicals form on a silica–alumina surface at undefined Lewis acid sites (*3*). The dependence of radical formation on oxygen uptake by the surface was studied to gain insight into the radical formation process (*4–7*). Hall and Dollish provided evidence that oxygen was the electron acceptor in systems of perylene on silica–alumina oxide and silica–alumina ze-

[1] To whom correspondence should be addressed at School of Chemical Sciences, University of Illinois, 506 S. Mathews Av., Urbana, IL 61801.

0021-9517/89 $3.00

olite surfaces (*6*). Clarkson, in the only previous ENDOR study of this system, provided support for this view by showing a correlation between the perylene β proton hyperfine coupling constant and the energy separation between antibonding π^* orbitals of O_2^- for a series of oxide surfaces (*8*). However, Garret *et al.* reported observation of an EPR signal due to an electron trapped at an $^{27}Al^{3+}$ site on systems of perylene on silica doped with 0.8% aluminum (*9*).

Characterization of the site itself has been equally elusive. Dollish and Hall proposed a mechanism for its formation in silica–alumina zeolites via dehydration of Brønsted acid sites (*5*). Meanwhile, Flockhart *et al.* showed that the site responsible for perylene radical formation in alumina is poisoned by Lewis bases (*10*). Later, he postulated two types of sites on the alumina surface, one in which the perylene is oxidized to the cation and subsequently combines with molecular oxygen to give a broad, featureless EPR signal, and one in which the oxygen cannot associate with the perylene, to give a signal with hyperfine splitting (*11*). Conversely, Wozniewski *et al.* concluded that, on a silica–alumina surface, a Brønsted acid site is responsible for the EPR signal with hyperfine structure whereas a Lewis acid site results in physical attachment between radical and surface and an EPR signal with no hyperfine structure (*12*). Alternatively, Muha has extracted information about the degree and type of motion of perylene on alumina and silica–alumina surfaces (*13*, *14*). With this and other information, he concluded that perylene radical *anion*, not the cation, is formed on alumina in a cooperative fashion between both donor and acceptor sites (*15*).

The studies cited have involved careful and often elegant chemical manipulation of the perylene–oxide surface system. However, in most cases the spectroscopic analysis has been limited to measurement of the intensity of the EPR signal and/or observation of the presence (or lack) of hyperfine structure. The problem with this approach is that the manipulated system is now chemically different from that for which the study was intended. It would be better if additional information could be extracted from the unaltered system.

This has been accomplished through a combination of investigative methods. ENDOR spectroscopy is used to detect magnetic nuclei in the vicinity of the perylene radical. In order to identify and determine the source of the signals, isotopic substitution is employed. In this way, these nuclei can be introduced to or removed from the sample through the least invasive of chemical manipulations. Finally, information about relative motion between the radical and its environment can be obtained, as explained later, by varying the temperature of the ENDOR experiment.

A double-resonance technique which depends on simultaneous excitation of both electron and nuclear spin transitions, ENDOR is inherently well suited to the detection of electron–nuclear hyperfine interactions. In addition to hyperfine interactions between the unpaired electron and nuclei chemically bonded to the perylene ring, there are also electron–nuclear through-space dipole–dipole interactions between the electron and more distant magnetic nuclei. These give rise to an effect called matrix ENDOR. In the text by Kevan and Kispert, the general lineshape of a matrix ENDOR line is described by the equation (*17*)

$$f(\upsilon) = k \int_a^r \int_0^\pi \int_0^{2\pi} R(r,\theta,\Phi) \times g(\upsilon - \upsilon_0(r,\theta,\Phi))\, r^2 \sin\theta\, dr\, d\theta\, d\Phi. \quad (1)$$

Here, a, the lower limit of the radial integral, represents an effective distance at which the matrix nuclei begin for which only a dipolar interaction is considered, k is a constant that affects the amplitude but not the shape of the line, and $g(\upsilon - \upsilon_0)$ is the nuclear spin packet lineshape centered at the resonant frequency υ_0. R is a function

of varying relaxation times that largely determines the ENDOR intensity. In general, this function contains terms taking into account the gyromagnetic ratio of the electron, γ_e, the gyromagnetic ratio of the particular nucleus involved, γ_n, and the distance between the nucleus and the electron (r^{-6} for common relaxation mechanisms), as well as terms defining the angular dependence between the electron and proton (*16*). We see therefore that matrix ENDOR intensity depends on environmental characteristics of the sample such as the type of nuclei present, the density of those nuclei, and the proximity of the nuclei to the electron.

In ring-proton ENDOR, the signals manifest themselves as pairs of resonance lines distributed symmetrically about the nuclear Larmor precessional frequency for protons. In matrix ENDOR, the magnitude of the hyperfine interaction is smaller than the peak linewidth, so the signals appear instead as *single lines at the Larmor frequencies* of the nuclei involved.

The intensities of these lines exhibit a marked temperature dependence. In addition to the influence of temperature on relaxation rates, which affects all ENDOR features through the $R(r,\theta,\Phi)$ term in Eq. (1), matrix interactions are directly affected by the relative motion between radical and environment. Motion in the system averages the dipole–dipole interactions, so one expects matrix ENDOR features to become significantly more intense if the relative motion between radical and environment is diminished. Thus the intensity of matrix peaks can be observed to increase strongly over some range of decreasing temperature. At some point, these motional effects will become frozen out and this intensity increase will no longer be observed. In this way, temperature can be used as a tool to probe the motion of the radical relative to the matrix nuclei in its environment. Therefore, ENDOR spectra have been recorded and are presented over a range of temperatures for each sample.

EXPERIMENTAL

Samples were prepared by injection of a solution of perylene in benzene or d_6-benzene onto an activated alumina or silica–alumina surface. Details of sample preparation are described in Paper I and will not be repeated here (*1*). Samples prepared from d_{12}-perylene (98%, MSD isotopes) were treated in the same manner. After recording their EPR and ENDOR spectra, we desolvated selected samples by overnight pumping on a vacuum line and again recorded their spectra. During this process, precautions were taken to avoid exposing the sample to light.

ENDOR and *X*-band EPR spectra were run on a Bruker ER-200D *X*-band EPR spectrometer equipped with an EN-810 ENDOR accessory, an Aspect 2000 computer for control and data acquisition, and variable temperature accessories for operating in liquid nitrogen or liquid helium temperature ranges, respectively. In general, spectra for a single sample were run at a variety of temperatures between 110 and 180 K using the nitrogen gas flow system. A second sample, prepared in the same manner, was then studied at helium temperature.

Optimum matrix ENDOR signals required low microwave power levels (usually 2 mW or less) coupled with large radio-frequency modulation depths (150–200 kHz). In contrast, the optimum ring-proton ENDOR signals appeared at microwave power levels of 5 mW or more. When spectra were run at liquid helium temperature, optimum microwave power levels were somewhat lower for both types of signals.

RESULTS

Expanded views of the ENDOR spectra obtained from a 0.002 *M* perylene solution on alumina under (protiated) benzene are shown in Fig. 1. At high gain, with the large proton matrix peak driven off scale, a signal is discovered at 3.7 MHz which is not attributable to perylene ring-proton hyperfine interactions. As the temperature is lowered

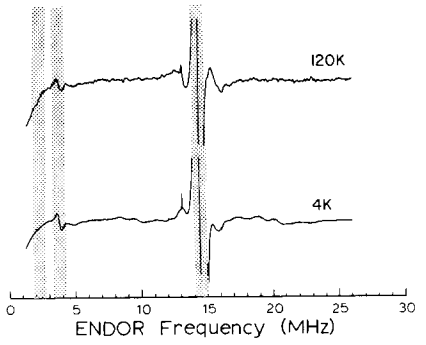

FIG. 1. ENDOR spectra of the perylene cation radical at 120 and 4 K obtained from irradiating in center of EPR spectrum. Both samples prepared by injection of a 0.002 *M* solution of perylene in benzene onto an activated alumina surface. Operating parameters as follows: microwave power = 0.8 mW (spectrum at 120 K) and 0.6 mW (spectrum at 4 K); rf power maximum (at amplifier meter) = 300–350 W; modulation depth = 200 kHz (spectrum at 120 K) and 150 kHz (spectrum at 4 K); ENDOR sweep rate = 1.25 MHz/s (spectrum at 120 K) and 1.5 MHz/s (spectrum at 4 K); time cnst. = 50 ms; 25 time-averaged scans (for spectrum at 4 K) minus an off-resonance background of an additional 25 scans (for spectrum at 120 K).

from 120 to 4 K, the intensity of this signal increases relative to the perylene hyperfine features, behavior which would be expected only for a matrix peak. No other features akin to this are observed in the low-frequency region of the ENDOR spectrum.

Figure 2 shows the ENDOR spectra of 0.002 *M* perylene in d_6-benzene on alumina at 180, 110, and 3 K. At each of these temperatures, there are features attributable to perylene ring-proton hyperfine couplings, plus three additional peaks, none of which has a mate or is otherwise part of a pair of hyperfine-split lines, and all of which grow stronger with decreasing temperature. In addition to the proton matrix line at 14.3 MHz, and the previously observed peak at 3.7 MHz, there is now an additional signal at 2.3 MHz.

When the d_6-benzene solvent was removed by evacuation (Fig. 3), the 2.3-MHz signal vanished while the peaks at 14.3 and 3.7 MHz remained. The evacuated sample which was used to record the spectra shown in Fig. 3 is the same as that for which the 180 and 110 K spectra are shown in Fig. 2. The matrix peaks in the evacuated sample, unlike the samples with frozen solvent, do not grow in intensity with decreasing temperature in the range 180 to 110 K.

In an effort to further determine the origin of the proton matrix peak in the samples under d_6-benzene, a sample was prepared with d_{12}-perylene under d_6-benzene on alumina. Figure 4 (^{1}H matrix region) shows the spectrum surrounding 14 MHz, normally containing proton-derived signals. A lone peak at 14.3 MHz contrasts starkly with the featureless background. Examination of the low-frequency region in Fig. 4 reveals the familiar 2.3 and 3.7-MHz signals interspersed among a group of previously unobserved features.

Contrasting with the spectra of samples

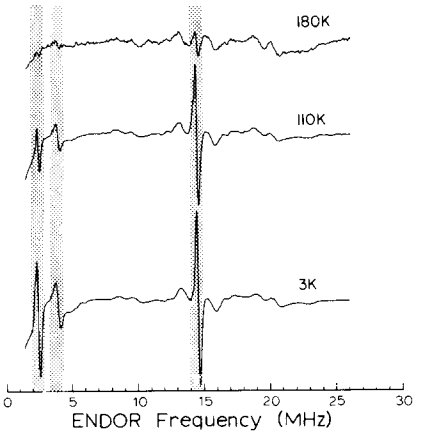

FIG. 2. ENDOR spectra of the perylene cation radical at 180 K, 110 K (same sample as 180 K), and 3 K obtained from irradiating in center of EPR spectrum. Samples prepared by injection of a 0.002 *M* solution of perylene in d_6-benzene onto an activated alumina surface. Operating parameters as follows: microwave power = 0.8 mW (180 K), 0.5 mW (110 K), and 0.2 mW (3 K); rf power maximum (at amplifier meter) = 300–350 W; modulation depth = 150 kHz (180 and 110 K) and 200 kHz (3 K); ENDOR sweep rate = 1.25 MHz/s (180 and 110 K) and 1.5 MHz/s (3 K); time cnst. = 50 ms; 25 time-averaged scans (for spectrum at 3 K) minus an off-resonance background of an additional 25 scans (for spectra at 180 and 110 K).

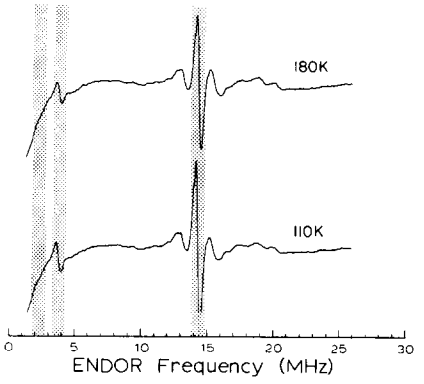

FIG. 3. ENDOR spectra of the perylene cation radical at 180 and 110 K obtained from irradiating in center of EPR spectrum. The sample is the same as that shown in Fig. 2 at 180 and 110 K after desolvating overnight on a vacuum line. Operating parameters as follows: microwave power = 4 mW (180 K), and 1 mW (110 K); rf power maximum (at amplifier meter) = 300–350 W; modulation depth = 200 kHz (both spectra); ENDOR sweep rate = 1.25 MHz/s (both spectra); time cnst. = 50 ms; 25 time-averaged scans minus an off-resonance background of an additional 25 scans.

recorded on an alumina surface are those of perylene in benzene and d_6-benzene on a silica–alumina surface, shown in Figs. 5 and 6. Under (protiated) benzene shown at 180, 110, and 5 K in Fig. 5, the 14.3-MHz proton matrix peak is still the largest feature in the spectrum, although the ring-proton hyperfine couplings are considerably more intense. With d_6-benzene as the solvent (Fig. 6) the proton matrix peak is not detectable at all, even near liquid helium temperature (6 K). The 2.3-MHz peak is very weak; it could be observed only upon close examination and expansion of the low-frequency region at 110 K. It is, however, easily detected at 6 K. The 3.7-MHz resonance was never observed on a silica–alumina surface under any conditions.

DISCUSSION

In the course of these experiments, three features were observed which are attributed to matrix interactions. Table 1 summarizes the existence and behavior of these features as a function of sample variation.

Paper I of this series (*1*) showed how the use of d_6-benzene as the solvent for deposition of perylene on oxide surfaces served to suppress the dominant proton matrix peak

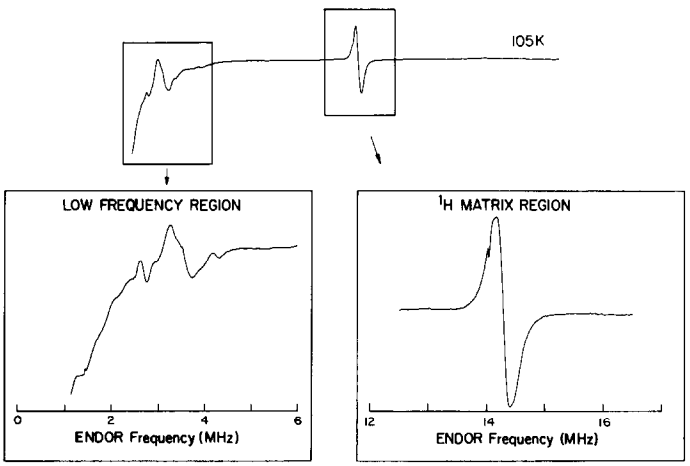

FIG. 4. ENDOR spectra of the perylene cation radical prepared by injection of a solution of d_{12}-perylene in d_6-benzene onto an activated alumina surface. All spectra obtained from irradiating in center of EPR spectrum at 105 K. Operating parameters are as follows: microwave power = 1 mW (all spectra); rf power maximum (at amplifier meter) = 350–450 W; modulation depth = 100 kHz (full-range spectrum and low-frequency inset) and 175 kHz (^{1}H matrix inset); ENDOR sweep rate = 1.5 MHz/s (full range), 0.25 MHz/s (low-frequency inset), and 0.20 MHz/s (^{1}H matrix inset); time cnst. = 100 ms; number of time-averaged scans = 17 (full range spectrum), 20 (low-frequency inset), and 10 (^{1}H matrix inset).

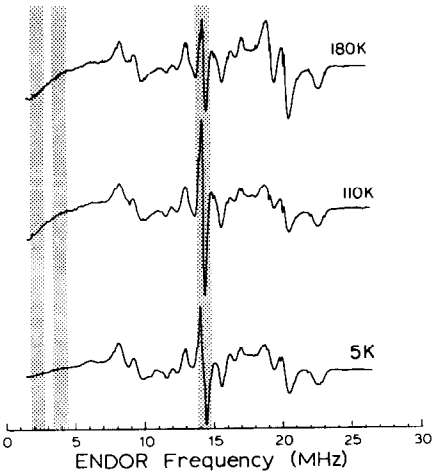

FIG. 5. ENDOR spectra of the perylene cation radical at 180 K, 110 K (same sample as 180 K), and 5 K obtained from irradiating in center of EPR spectrum. Samples prepared by injection of a 0.001 *M* solution of perylene in normal (protiated) benzene onto an activated silica–alumina surface. Operating parameters as follows: microwave power = 13 mW (180 K) and 8 mW (110 and 5 K); rf power maximum (at amplifier meter) = 250–350 W; modulation depth = 150 kHz (all spectra); ENDOR sweep rate = 1.5 MHz/s (all spectra); time cnst. = 20 ms (180 and 110 K) and 50 ms (5 K); 25 time-averaged scans (for spectra at 110 and 5 K) minus an off-resonance background of an additional 25 scans (for spectrum at 180 K).

and thus simplify the study of the perylene ring proton hyperfine features. It was explained that, as the proton matrix signal was due principally to an interaction between the unpaired electron and solvent protons, it diminished when the benzene was deuterated. However, under instrumental conditions favorable to matrix features (see Experimental), this signal is not completely suppressed; in fact it can be seen even at 180 K (Fig. 2). As the temperature is lowered to 110 and 3 K, the peak grows in intensity, as would be expected from a decrease in motional averaging (see Introduction and Table 1). At these lower temperatures, the proton matrix peak is the most intense feature in the spectrum, despite the fact that the solvent contains no hydrogen. In addition, two other peaks are observed, at 2.3 and 3.7 MHz, whose microwave power and temperature dependence are clearly consistent with those of matrix features. The signal at 3.7 MHz is also observed in the spectra of perylene on alumina under (protiated) benzene, while the 2.3-MHz signal is not (see Table 1 and Fig. 1).

In the following discussion, two questions brought about by these observations are answered. First, the identity of the new matrix features is established. Also, the source (or sources) of intensity for the proton matrix peak when the sample is under d_6-benzene is identified.

Identity of 2.30 and 3.7-MHz Signals

It is no surprise that the peak at 2.3 MHz falls at the nuclear precession frequency expected for deuterium, an assignment consistent with all the experimental observations. However, the peak at 3.7 MHz falls close to the free nuclear precession frequency of a large number of magnetic nuclei in the periodic table. Of all the possibilities, only two, aluminum-27 and carbon-13, can reasonably be expected in the perylene–solvent–surface system. At the experimental magnetic field of 0.3347 T, the ENDOR signals for these nuclei would lie at 3.71 and 3.58 MHz, respectively. Since this difference is within the linewidth of the observed peak, evidence other than frequency must be used for an assignment. However, the fact that aluminum-27 is the sole naturally occurring aluminum isotope while carbon-13 represents but 1.1% of all carbon isotopes suggests assignment of this signal partly or wholly to aluminum-27. Arguments based on substrate composition and evacuation of solvent (vide infra) also support this assignment.

In the ENDOR spectra of perylene on alumina under (protiated) benzene acquired under normal operating conditions, the proton matrix peak strongly dominates the spectrum; no other matrix features are detectable. However, when the gain is increased so as to drive the 14.3-MHz peak off scale (Fig. 1), the 3.7-MHz feature is

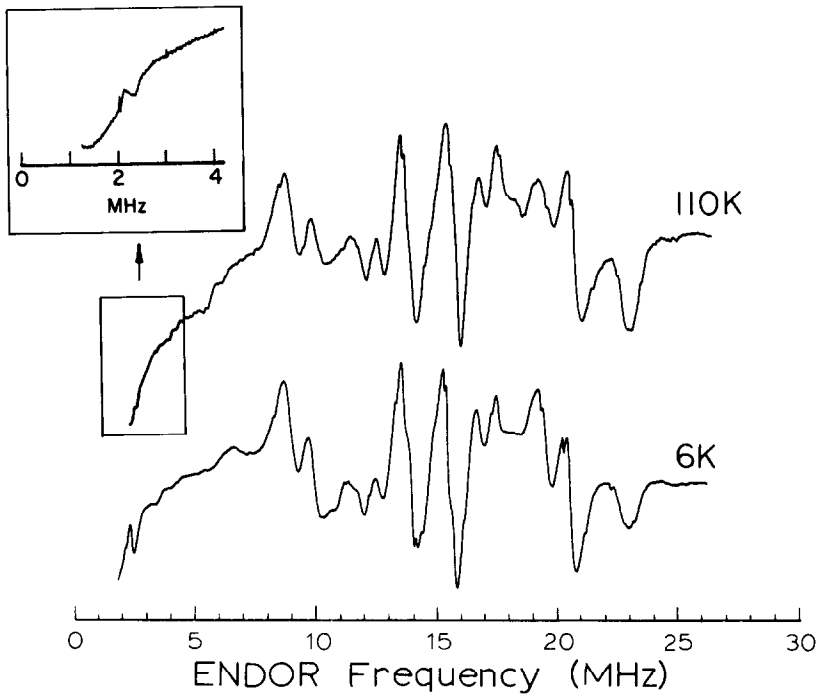

FIG. 6. ENDOR spectra of the perylene cation radical at 110 and 6 K obtained from irradiating in center of EPR spectrum. Samples prepared by injection of a 0.001 *M* solution (110 K full range and 6 K spectra) or 0.002 *M* (110 K inset) of perylene in d_6-benzene onto an activated silica–alumina surface. Operating parameters as follows: microwave power = 8 mW (110 K full range), 1 mW (110 K inset), and 3 mW (6 K); rf power maximum (at amplifier meter) = 250–350 W (110 K full range and 6 K) and 300–400 W (110 K inset); modulation depth = 150 kHz (all spectra); ENDOR sweep rate = 1.5 MHz/s (110 K full range and 6 K) and 0.5 MHz/s (110 K inset); time const. = 50 ms (110 K full range and 6 K) and 20 ms (110 K inset); 25 time-averaged scans with no background subtracted (110 K full range and 6 K), 50 time-averaged scans minus an off-resonance background of an additional 50 scans (110 K inset).

TABLE 1

Summary of Matrix Peak Observation

Sample	Matrix feature		
	14.3-MHz peak	3.7-MHz peak	2.3-MHz peak
pery(+) on Al_2O_3 under C_6H_6	Very strong	Present, strong near He temp	Missing
pery(+) on Al_2O_3 under C_6D_6	Strong, especially at lower temps	Present, strong near He temp	Present, strong near He temp
pery(+) on Al_2O_3 evacuated	Strong, constant w/ temp	Present, constant w/temp	Missing
d_{12}-pery(+) on Al_2O_3 under C_6D_6	Strong	Present	Present
pery(+) on Si–Al oxide under C_6H_6	Strong	Missing	Missing
pery(+) on Si–Al oxide under C_6D_6	Missing	Missing	Weak, except near He temp
d_{12}-pery(+) on Si–Al oxide under C_6D_6	Very weak	Missing	Many features present in region

visible and increases in intensity as the temperature is reduced from 120 to 3 K (see Table 1), as would be expected for either aluminum-27 or carbon-13 in the matrix. On the other hand, no peak is observed at 2.3 MHz, even at liquid helium temperature, in accord with its assignment to solvent deuterium in Fig. 2.

Our silica–alumina substrate is Houdry M-46, a commercial catalyst containing roughly 90% silica and 10% alumina. It is therefore expected that if the 3.7-MHz signal is due to aluminum-27, it would be greatly diminished or missing, while a carbon-13 derived matrix peak would be relatively unaffected. An inspection of the ENDOR spectra on silica–alumina (see Table 1 and Figs. 5 and 6) shows the former to be true. Although all of the matrix peaks are less intense on this surface, the 2.3-MHz deuterium signal (the intensity of which was similar to that of the 3.7-MHz peak for the spectra on alumina) behaves as expected, while no signal could ever be detected at the 3.7-MHz frequency.

In the evacuated alumina-bound perylene sample which exhibits the spectrum of Fig. 3, all the solvent has been pumped off in order to eliminate it as a possible source of protons, deuterons, or carbon. As expected, the 2.3-MHz deuterium matrix peak vanishes with the removal of the deuterated solvent. However, the other two matrix peaks remain, indicating little disruption of the sites from which they are derived. Again, this is consistent with the assignment of the 3.7-MHz peak to aluminum-27, which would be relatively unaffected by solvent evacuation. If this peak were due to carbon-13, one would expect a major perturbation on the system due to removal of over 99% of the carbon present upon evacuation of the sample.

In addition to providing strong evidence as to the assignment of the 3.7-MHz feature to aluminum-27, the evacuated sample illustrates a different temperature dependence. Under frozen solvent, an increase in intensity of the matrix peaks is observed with a decrease in temperature (e.g., Fig. 1 or 2). This behavior may be attributed to a slowing of the molecular motion which would otherwise average to zero the dipole–dipole interactions which result in matrix ENDOR features. In contrast, the spectra of the evacuated sample (Fig. 3) show virtually no intensity changes in matrix features between 180 and 110 K. There is obviously less relative motion between the perylene radical and its environment. At least two explanations suggest themselves: (i) the primary source of motion in the samples under frozen benzene is the frozen solvent, or (ii) the lack of solvent in the evacuated sample forces the perylene radical into a closer interaction with the surface, hindering motion. In either case, the perylene radical in the evacuated samples behaves as if immobilized, even at 180 K.

Source of the 14.3-MHz Proton Matrix Signal

Earlier, it was observed that a substantial proton matrix feature appeared in the ENDOR spectrum even if the samples contained deprotonated solvent (see Table 1 or Fig. 2) or no solvent (see Table 1 or Fig. 3). In these samples, the proton matrix peak must originate with hydrogen nuclei located in either (i) the alumina surface or (ii) unreacted (nonradical) perylene molecules. The latter possibility is excluded when both deuterated perylene and deuterated benzene are used to prepare a sample on alumina. The proton matrix region of the ENDOR spectrum (Fig. 4) no longer contains perylene ring-proton hyperfine couplings, a fact indicating that no processes have taken place to exchange protons with the surface—yet the proton matrix peak itself remains (see Table 1). This indicates an interaction between adsorbed perylene radical and protons which must be located in the alumina on or near the surface. Note that this does *not* imply that the surface is the sole source of protons in the vicinity of

the radical, but rather that the surface must be at least a contributing source.

A closer examination of the low-frequency region of this sample (Fig. 4) again reveals the presence of the now-familiar deuterium and aluminum-27 peaks at 2.3 and 3.7 MHz. However, they are now joined by a new set of couplings arising from deuterium in the d_{12}-perylene itself. Assignment of these features to specific ring positions is complicated by several factors which arise from the small deuterium nuclear precession frequency and high spin ($I = 1$), as well as some instrumental difficulties in recording spectra at very low frequencies. Accordingly, we present no assignments here; however, we expect to modify our computer simulation program (*1*) later to handle the theoretical complications.

Comparison of Alumina and Silica–Alumina Surfaces

While the ENDOR spectra of perylene adsorbed on our activated *alumina* surfaces exhibit a variety of intense matrix features, the ENDOR of perylene on our *silica–alumina* surface (Figs. 5 and 6) is nearly devoid of matrix effects. The matrix intensity on the silica–alumina surface, measured with respect to the intensity of the EPR signal, is roughly an order of magnitude weaker than the corresponding alumina surface. Although the 14.3-MHz proton matrix peak is still the largest signal in the spectrum of perylene on silica–alumina under (protiated) benzene (Fig. 5), the signal does not dominate the spectrum as do the matrix peaks in Fig. 1. With d_6-benzene as the solvent (Fig. 6), there is no detectable matrix peak even at 6 K (see Table 1). This should be contrasted with Fig. 2, where the proton matrix peak becomes the largest feature in the spectrum as high as 110 K under d_6-benzene. Under conditions of 110 K temperature, high spectrometer gain, and many time-averaged scans, a matrix deuterium signal at 2.3 MHz barely rises out of the noise (Fig. 6 inset) in contrast to the easily visible 2.3-MHz feature in Fig. 2. The 3.7-MHz aluminum-27 matrix peak, the intensity of which was similar to that of the deuterium matrix signal in the ENDOR or perylene on alumina, cannot be observed in this spectrum or under any other conditions on those samples on a silica–alumina surface (see Table 1).

These observed intensity differences can be traced to differences in one of the following factors: (i) the nature of the radical itself on the two surfaces; (ii) the number and distances of magnetic nuclei surrounding the radical; (iii) the degree of motional averaging on the two surfaces; or (iv) differences in relaxation due to environmental differences.

We rule out (i) because the agreement of the values of the anisotropic perylene ring-proton hyperfine couplings implies that the radicals formed on the two surfaces are similar (*1*). We cannot rule out (iii) at higher temperatures, but near liquid helium temperature the degree of motional averaging should be near zero on both surfaces—yet the differences in matrix intensity remain. This leaves (ii) and (iv), which are not easily distinguishable and may be interrelated. However, the common theme of both factors is that this difference in intensity of matrix features of the perylene radical on alumina vs silica–alumina surfaces can be attributed to a *difference in environment* of the respective radicals.

The data indicate that on the alumina surface, the radical has stronger interactions and/or less mobility relative to its environment than it has on the silica–alumina. Specifically, our alumina surface is marked by spectroscopic evidence of the ubiquitous proton while our silica–alumina is not (see Table 1). Also, the perylene radical on our alumina rests near at least one aluminum atom; the typical detection range of matrix ENDOR is limited to within 5 to 6 Å (*17*). Conversely, the aluminum-27 resonance is never observed with our Houdry M-46 silica–alumina material (see Table 1). Even if we postulate that, after formation, the

perylene cation radical migrates on the surface so as to establish an equilibrium surface coverage without regard to specific sites, we must recognize that the Houdry M-46 catalyst still has a substantial Al content (12% Al_2O_3 and 88% SiO_2). Thus, by analogy to the results obtained on pure alumina, one would still expect that an aluminum-27 matrix ENDOR line in the Houdry M-46 samples could be detected at liquid helium temperatures, providing that the aluminum–radical distances are about the same on the two surfaces. The absence of this spectral feature from the silica–alumina surface thus is significant. These observations support a model in which the cation radical is relatively immobile at a surface site whose composition includes protons and aluminum. Such site characteristics seem to agree well with the Al^{3+} (cus) site on partially dehydroxylated alumina proposed by Burwell (*19*) and reviewed by Knözinger (*20*).

The lack of aluminum-27 and strong proton signals in the ENDOR spectra of perylene on the silica–alumina is more puzzling. In a recent review of quantum chemical cluster models for acid–base sites on metal oxides, Zhidomirov and Kazansky note that oxygen anions in a noncrystalline silica–alumina oxide lattice would be expected to exert a fairly strong screening effect on adsorbate molecules approaching a trigonal aluminum Lewis acid site (*21*). Their model agrees in its main features with those proposed by Uytterhoeven *et al.* (*22*) and Stamires and Turkevich (*23*) for Lewis acid sites on zeolites. One consequence of such site geometry would be to prevent an extremely close approach of the adsorbed radical to aluminum atoms. Since the amplitudes of matrix ENDOR transitions depend critically on the electron–nuclear distance, **r** (the dependence is r^{-6}), the spectroscopic effect of a larger radical–aluminum distance would be the presence of aluminum matrix ENDOR signals in alumina samples and their absence from the Houdry M-46 case. This observation may thus be a reflection of differences in **r** for the two systems, caused by different acid site geometries.

Differences in proton matrix ENDOR intensities between the two systems also may be a function of different surface structures. As Table 1 summarizes, proton matrix intensity from solvent protons is weaker for silica–alumina samples than for alumina. At temperatures above the lowest ($T > 10$ K), this may be due to a greater surface mobility for molecules adsorbed on silica–alumina surfaces, producing a partial averaging of the dipole–dipole coupling terms in Eq. (1). The extremely weak matrix ENDOR intensity from surface protons on silica–alumina at low temperatures ($T < 10$ K) where surface mobility should be quenched is quite surprising, since one would expect surface hydrogen to be present. Only three variables control such an intensity effect: (i) electron–nuclear distance, **r**; (ii) proton density; and (iii) electronic and nuclear relaxation. In general, the proportionality relationship between ENDOR intensity and number (or density) of nearby magnetic nuclei is invalid when comparing two different samples since the relaxation mechanisms, which also determine ENDOR intensity, are influenced by environmental sources. However, it seems unlikely that spin relaxation in this system is sufficiently different from the alumina case to quench matrix ENDOR intensity. Therefore the environment of perylene radical on the silica–alumina surface must be such that either electron–proton distances are large or the radical adsorbs preferentially in regions of low proton density. Further work is under way in our laboratory to attempt to clarify this question.

CONCLUDING REMARKS

That observation of matrix ENDOR features together with isotopic substitution of magnetic nuclei has provided valuable insight into the environment of radicals adsorbed on metal oxide surfaces. The information obtained has complemented our

earlier study. While the ring-proton hyperfine couplings, analyzed in Paper I (*1*), provided evidence that the *identities* of the perylene radicals on the two surfaces studied are similar, the matrix hyperfine features reported on here indicate that the *environments* of the radical are different.

For other systems, it has been shown that one can model the lineshape of the matrix line and obtain information about the number of nuclei of a specific type neighboring the radical (*18*). We are proceeding to apply these methods to our perylene radicals–oxide surface ENDOR spectra in order to derive quantitative information from our data. The results of this effort will be reported in a subsequent paper.

ACKNOWLEDGMENTS

This research is supported by grants from the U.S. Department of Energy (DOE DEFG 22-84PC70782, Pittsburgh Energy Technology Center); Illinois Department of Energy and Natural Resources, Coal Development Board, through CRSC; U.S. National Institute of Health (RR01811, Division of Research Resources); and the Petroleum Research Fund administered by the American Chemical Society. We gratefully acknowledge the cooperation in the performance of experiments by Professor Peter G. Debrunner (Physics Department, University of Illinois at Urbana–Champaign).

REFERENCES

1. Clarkson, R. B., Belford, R. L., Rothenberger, K. S., and Crookham, H. C., *J. Catal.* **106,** 500 (1987).
2. Rooney, J. J., and Pink, R. C., *Proc. Chem. Soc.*, 70 (1961).
3. Hall, W. K., *J. Catal.* **1,** 53 (1962).
4. Flockhart, B. D., Scott, J. A. N., and Pink, R. C., *Trans. Faraday Soc.* **62,** 730 (1966).
5. Dollish, F. R., and Hall, W. K., *J. Phys. Chem.* **71,** 1005 (1967).
6. Hall, W. K., and Dollish, F. R., *J. Colloid Interface Sci.* **26,** 261 (1968).
7. Imai, H., Ono, Y., and Keii, T., *J. Phys. Chem.* **69,** 1082 (1965).
8. Clarkson, R. B., *Magn. Reson. Colloid Interface Sci.*, 425 (1980).
9. Garret, B. R. T., Leith, I. R., and Rooney, J. J., *Chem. Commun.*, 222 (1969).
10. Flockhart, B. D., Sesay, I. M., and Pink, R. C., *J. Chem. Soc. Faraday Trans. 1* **79,** 1009 (1983).
11. Flockhart, B. D., and Salem, M. A., *J. Colloid Interface Sci.* **103,** 76 (1985).
12. Wozniewski, T., Fedorynska, E., and Malinowski, S., *J. Colloid Interface Sci.* **87,** 1 (1982).
13. Muha, G. M., *J. Phys. Chem.* **71,** 633 (1967).
14. Muha, G. M., *J. Chem. Phys.* **67,** 4840 (1977).
15. Muha, G. M., *J. Catal.* **58,** 470 (1979).
16. Hyde, J. S., Rist, G. H., and Eriksson, L. E. G., *J. Phys. Chem.* **72,** 4269 (1968).
17. Kevan, L., and Kispert, L. D., "Electron Spin Double Resonance Spectroscopy." Wiley–Interscience, New York, 1976.
18. Narayana, P. A., Bowman, M. K., Becker, D., Kevan, L., and Schwartz, R. N., *J. Chem. Phys.* **67,** 1990 (1977).
19. Burwell, R. L., Jr., *J. Catal.* **86,** 301 (1984).
20. Knözinger, H., "Catalysis by Acids and Bases," pp. 11–125. Elsevier, Amsterdam, 1985.
21. Zhidomirov, G. M., and Kazansky, V. B., "Advances in Catalysis" (D. D. Eley, P. W. Selwood, and P. B. Weisz, Eds.), Vol. 34, p. 131. Academic Press, New York, 1986.
22. Uytterhoeven, J. B., Christner, L. G., and Hall, W. K., *J. Phys. Chem.* **69,** 2117 (1965).
23. Stamires, D. N., and Turkevich, J., *J. Amer. Chem. Soc.* **86,** 749 (1964).